

# Assessment of relative density on shear strength and volumetric characteristics of sand-EPS particulate mixtures

Mahmood Reza Abdi<sup>1\*</sup>, Ali Khakbazan<sup>2</sup>, Maryam Kazemi Abyaneh<sup>3</sup> and Mahdi Safdari Seh Gonbad<sup>4</sup>

<sup>1</sup>Associate Professor, Civil Engineering Faculty, K.N. Toosi University of Technology, Tehran, Iran.

Email: [abdi@kntu.ac.ir](mailto:abdi@kntu.ac.ir) - Mobile Number

Address: No. 1346, Valiasr Street, Mirdamad Intersection, Tehran, Iran. <https://orcid.org/0000-0002-3473-9677>

<sup>2</sup>Assistant Professor, Water-Soil Department, Imam Khomeini Higher Education Center, Karaj, Iran.

Email: [a.khakbazan@itvhe.ac.ir](mailto:a.khakbazan@itvhe.ac.ir) – Mobile Number:

<sup>3</sup>Geotechnical Postgraduate, Civil Engineering Faculty, K.N. Toosi University of Technology, Tehran, Iran.

Email: [kazemi.abbyaneh.73@gmail.com](mailto:kazemi.abbyaneh.73@gmail.com) – Mobile Number:

<sup>4</sup>Geotechnical Postgraduate, Civil Engineering Faculty, K.N. Toosi University of Technology, Tehran, Iran.

Email: [m.safdari@email.kntu.ac.ir](mailto:m.safdari@email.kntu.ac.ir) – Mobile Number: <https://orcid.org/0000-0003-0612-535X>

## Abstract

Geofoam is widely used in civil engineering projects due to its low unit weight, insensitivity to moisture variations and high erosion resistance. In present study, the effect of expanded polystyrene (EPS) particulates on the shear strength and volumetric characteristics of sand has been investigated using direct shear test. Sand has been mixed with 0.1, 0.2 and 0.3% EPS as dry weight of soil and compacted to relative densities ( $R_d$ ) of 60, 65, 70, 75 and 80% in a shear box 60×60×26 mm and subjected to normal pressures of 100, 200 and 300 kPa. Results showed that by the addition of geofoam particulates to sand, shear strength characteristics such as cohesion, angle of internal friction and dilation as well as the stiffness of the mixtures decreased resulting in overall reduction of the shear strength. Increasing the relative density of sand-geofoam particulate mixtures, reversed the changes in the preceding characteristics. Shear strength and stiffness of samples improved with increase in normal pressure whereas dilation angles decreased. Cohesions displayed by samples are apparent and attributed to the penetration of sand particles into geofoam particulates resulting in particle confinement and thus reduction of dilation.

**Keywords:** Direct shear, Sand, Geofoam particulates, Relative density, Dilation.

## 1. Introduction

Expanded polystyrene (EPS) geofoam is a super-lightweight rigid cellular polymeric material with a density of about 1% of that of soil [1]. Geofoams are used as lightweight fillers to improve geotechnical characteristics and to reduce unit weight of soils [2, 3, 4, 5 & 6]. Lightweight materials are used as backfill of retaining structures to reduce lateral pressures, embankments to reduce driving forces, as seismic buffers to alleviate forces on retaining

32 walls, in pavements to reduce noise, in pipeline trenches, etc. [7, 8, 9, 10, 11, 12, 13, 14, 15, 16, 17, 18 & 19].  
33 Inclusion of lightweight material to cohesion-less soils increases damping ability to absorb dynamic stresses and  
34 reduce forces imposed on retaining walls, buried pipes, etc. [20, 21 & 22]. Researchers have investigated the effects  
35 of lightweight fill materials such as tire (rubber) and plastic strip wastes as well as EPS geof foam blocks on soil  
36 behavior.

37 Miki (1996) conducted direct shear tests to determine interface friction coefficient between geof foam-geof foam  
38 and geof foam-sand and reported coefficients ranging from 0.55 to 0.7 [23]. Horvath (1997) based on laboratory test  
39 results, divided stress-strain behavior of soil-geof foam mixtures into linear elastic, plastic with specified yield  
40 strength, linear and nonlinear hardening parts [1]. Negussey (1997) reported that friction at sand-geof foam interface  
41 is comparable to the angle of internal friction of sand alone [24]. Chrysikos et al. (2006) conducted direct shear tests  
42 to measure frictional resistance at the interface of geof foam blocks with densities of 15 and 30 kg/m<sup>3</sup> and materials  
43 such as concrete, soils, geomembranes, and geotextiles [25]. Liu et al. (2006) investigated the influence of  
44 polystyrene pre-puff beads/soil (PSPP/S) weight ratios and showed unit weights to vary between 7 to 11 kN/m<sup>3</sup> [26].

45 Abdelrahman et al. (2008) reported that increase in the normal stress and decrease in geof foam density cause an  
46 increase in both the peak and residual friction coefficients of EPS blocks [27]. Kim et al. (2008) showed that  
47 inclusion of EPS particulates results in reducing the unit weights to 6 to 15 kN/m<sup>3</sup> [28]. Deng and Xiao (2010)  
48 studied the stress-strain behavior of EPS particulate-sand mixtures and showed decrease in strength with increasing  
49 EPS content with mixtures being 26 to 63% lighter than earth fill materials [29]. Heydarian et al. (2012) reported  
50 that the addition of geof foam particulates to sandy soils resulted in decrease of internal friction angle and increase of  
51 apparent adhesion and increased uniaxial compressive in clayey soils [30]. Rocco and Luna (2013) investigated the  
52 undrained shear strength of clay-EPS mixtures in saturated and unsaturated conditions. Results indicated that  
53 undrained shear strengths of saturated mixtures were unaffected whereas for partially saturated mixtures, EPS  
54 content caused significant reduction [31].

55 Padade and Mandal (2014) by blending fly ash with EPS particulates and cement and reported that the  
56 compressive strength of expanded polystyrene-particulates geomaterial increases considerably if cement-to-fly ash  
57 ratios of 10, 15 and 20% were used. Compared with EPS block geof foam, EPS particulates mixed geo-material  
58 showed higher density, compressive strength and stiffness which is suitable as fill material [32]. Effects of EPS  
59 particulates gradation on the stress-strain behavior of EPS-sand mixtures was investigated by Edinçililer and Özer  
60 (2014). Results showed that deviatoric stress of EPS-sand mixture is a function of EPS particulate content and size  
61 distribution [33].

62 Padade and Mandal (2014) investigated the interaction between geof foam-geof foam, geof foam-geotextile and  
63 geof foam-geogrid using EPS blocks 0.15, 0.2, 0.22 and 0.3 kN/m<sup>3</sup> in density and reported that shear strengths at  
64 interface is not significantly influenced by density of geof foam [34]. Özer and Akay (2016) by conducting direct  
65 shear tests on EPS blocks reported that shear strength is mainly dependent on its cohesion while interface shear  
66 strength is dependent on both adhesion and friction coefficient [35]. Direct shear tests were also conducted on  
67 geof foam-sand interface by AbdelSalam and Azzam (2016) and no significant change in interface friction coefficient

68 especially under low normal stress was observed in both dry and wet conditions [36]. Khan and Meguid (2018)  
69 showed that geofom-sand interface developed frictional resistance that is much larger than measured for geofom-  
70 PVC interface [37].

71 Dynamic properties of sand-EPS particulate mixtures were evaluated using resonant column and cyclic triaxial  
72 tests at small and large strains by El-Sherbiny et al. (2018). Results indicated a decrease in shear stiffness with  
73 increasing EPS content at all strain levels. Material damping was relatively unaffected at small and increased at  
74 larger strains [38]. Alaie and Jamshidi Chenari (2018) also conducted investigated dynamic properties of EPS-sand  
75 mixtures and reported damping of EPS-sand mixtures to increase with increasing EPS content [39]. In a later study  
76 Alaie and Jamshidi Chenari (2019,2020) by conducting cyclic triaxial tests on EPS-sand mixtures showed that shear  
77 velocity and modulus decrease with increasing EPS content and damping ratio decreases during the initial loading  
78 cycles and levels off afterwards [40,41]. Nawghare and Mandal (2020) and Ali et al. (2023) studied fly ash - EPS  
79 mixtures and reported that smaller EPS particulates proved more effective on improving shear strength than larger  
80 EPS particulates [42 & 43]. Abbasimaedeh et al. (2021) studied behavior of uncemented EPS -clayey soil mixtures  
81 as lightweight fill and reported that EPS beads caused substantial mechanical failure in direct shear with drastic  
82 decay of CBR and compressibility parameters [44]. Alaie et al. (2021) studying EPS-sand mixtures using laminar  
83 box on shaking table showed that deformations under dynamic loading were reduced and that the damping ratio and  
84 shear modulus depend on the EPS bed content [45].

85 Zhu et al. (2022) conducted dynamic triaxial tests on sand-EPS (LSES) mixtures and control sand (CS) and  
86 stated that dynamic strength of LSES decreased with the increase in EPS particulates content due to the low strength  
87 and smooth surfaces of EPS particulates [46]. Ge et al. (2022) investigated the shear performance of the sand-EPS  
88 mixtures at different moisture contents. Results showed that with increase in moisture content, the shear strength and  
89 the internal friction angle of sand-EPS mixtures initially decreased and then increased whereas cohesion increased  
90 first and then decreased [47]. Jili et al. (2022) explored the resistance characteristics of Shanghai clay-EPS mixtures  
91 and showed that with increase in EPS particle size, the compressive strength, compression and rebound index  
92 together with ductility of mixtures increased [48].

93 Bekranbehesht et al. (2023) investigated the influence of EPS beads on the shear stiffness of quartz and  
94 calcareous based materials using bender element tests and reported that maximum shear modulus increases with  
95 confining pressure and decreases with increasing void ratio and EPS content [49]. Tao et al. (2023) evaluating the  
96 dynamic modulus and damping characteristics of modified expanded polystyrene lightweight soil and reported that  
97 EPS content plays a decisive role on elastic modulus and damping ratio of the mixture [50]. Karimpour-Fard et al.  
98 (2023) evaluating compressibility of EPS beads and EPS-sand mixtures using triaxial tests, reported better  
99 agreement between CD and CU stress paths when EPS compressibility is considered [51]. Demiröz & Diker (2023)  
100 investigating the geotechnical properties of fill-EPS-waste tire observed that strength increased with increase in  
101 cement ratio, and decreased with EPS ratio and waste tires were found to have no impact on strength [52].  
102 Karademir (2023) investigated soil type and loading condition effects on soil-geofom interactions and reported that  
103 peak and residual shear stresses increased with increase in normal stress and granular compared with cohesive soil

104 demonstrated larger frictional strengths and the higher the granular soil angularity, the larger the interface shear  
105 strength [53].

106 Considering previous investigations, it is seen that effects of relative density as an influential factor on sand-EPS  
107 particulate mixtures has not formerly been assessed. Thus, in current research the influence of this factor on shear  
108 strength parameters, stress-strain and volumetric characteristics of sand-EPS particulate mixtures has been  
109 investigated. For this purpose, sand has been mixed with 0.1, 0.2 and 0.3% EPS particulates as dry weight of soil  
110 and compacted to 60, 65, 70, 75 and 80% of the sand maximum dry density. Samples 60×60×26 mm was prepared  
111 in slightly moist condition and tested using direct shear test with normal pressures of 100, 200 and 300 kPa.

## 112 **2. Experimental study**

### 113 **2.1. Materials**

#### 114 **2.1.1. Sand**

115 Due to suitable drainage characteristics and insensitivity to moisture variations, granular soils are mostly used as  
116 fill behind retaining walls [54, 55, 56, 57, 58, 59, 60 & 61]. Thus, in current research to be in accord with previous  
117 investigators a sandy soil has been selected for the investigations. The sand used was collected from Shahriar mines  
118 west of Tehran which are the main source of sand for civil engineering projects. Summary of the sand characteristics  
119 are presented in Table 1 with its maximum and minimum dry unit weights and the particle size distribution  
120 determined according to ASTM D4253 (2016), ASTM D4254 (2016) and ASTM D6913 (2017) respectively [62, 63  
121 & 64]. Considering Figure 1, it is observed that the soil comprises of 99% sand particle. According to Unified Soil  
122 Classification System (USCS) sand is grouped as SP (poorly graded sand) [65].

#### 123 **2.1.2. EPS particulates**

124 The EPS particulates used was obtained from a regional supplier of EPS materials for engineering,  
125 manufacturing, and packaging industries. EPS particulates are used to produce geofoam blocks 2000×500×250 mm  
126 with a density of 12 kg/m<sup>3</sup> with particulates varying in size from 2 to 5 mm. EPS particulates used is portrayed in  
127 Figure 2 with the physical and mechanical properties shown in Table 2 [66].

### 128 **2.2. Apparatus**

129 Direct shear test is the simplest method used for determination of granular soil shear strength characteristics as  
130 depicted in Figure 3. In current research, direct shear tests were conducted in accordance with the specifications  
131 outlined by ASTM D3080 [67]. Shear box 60×60×26 mm was adopted for the preparation of the samples and shear  
132 load was applied at a rate of 1 mm/min. During tests, horizontal and vertical displacements were measured  
133 employing LVDTs, and a load cell together with an automatic data recording system to measure and record shear  
134 force and displacements. Shear stresses presented have been calculated implementing modified shear surface areas.

### 135 **2.3. Sample preparation**

136 Samples were prepared by mixing sand with 0.1, 0.2 and 0.3% EPS particulates as dry weight of soil.  
137 Constituents were slightly moistened (<3%) to facilitate mixing and prevent segregation of EPS particulates.

138 Moistening helped EPS particulates to be more uniformly distributed in the mixture. Mass based proportions of  
139 sand and EPS particulates for different compositions and relative densities were determined and are presented in  
140 Table 3. Constituents were thoroughly mixed using an electric mixer until a homogeneous mixture was achieved.  
141 Samples were prepared and compacted on a separate table and subsequently transferred to the direct shear test  
142 apparatus. Samples were compacted to relative densities of 60, 65, 70, 75 and 80% (Fig. 4 (a)) and to be in accord  
143 with previous researchers subjected to normal pressures of 100, 200 and 300 kN/m<sup>2</sup>. These relative densities were  
144 adopted so the behavior of the sand-EPS mixtures could be assessed over a wide range of compaction degrees from  
145 medium to dense. Due to heterogeneity all tests were repeated 3 times.

146 To determine shear strength parameters of the geofoam, a series of direct shear tests were conducted on geofoam  
147 cubic specimens 60×60×26 mm as shown in Fig. 4 (b). The samples were subjected to the same normal pressures as  
148 soil-EPS particulate mixtures and the results were used to help interpret the shear stress-shear displacement and  
149 volumetric characteristics of the composite mixtures.

### 150 **3. Results and discussions**

#### 151 **3.1. Expanded polystyrene samples (EPS)**

152 To determine shear strength characteristics of the expanded polystyrene, 9 direct shear tests were conducted on  
153 cubic samples cut out of EPS blocks (i.e. geofoams). As the results obtained were very close, variations of shear  
154 stress-horizontal displacements for only a set of three samples are presented as representative in Fig. 5. It is  
155 observed that shear stresses continuously increase up to the maximum horizontal displacement of 7 mm which is  
156 equivalent to approximately 12% strain with no distinct failure points. The rate of variations in shear stresses with  
157 horizontal displacement show two distinct phases. During the first phase which starts from the beginning to a  
158 horizontal displacement of 1 mm (1-2% strain), the rate of increase in shear stresses is relatively high and thereafter  
159 the second phase starts exhibiting lower rate of increase in shear stresses. Due to the compressible nature of the EPS  
160 block, even after 12% strain the trend of changes show that the sample is being constantly compressed and becomes  
161 slightly stronger. Results show that even EPS samples subjected to higher normal pressures display greater shear  
162 stresses at a particular horizontal displacement. Effects of normal pressure at early stages of the tests are marginal  
163 and become intensified at greater horizontal displacements because the sample becomes compressed and  
164 consequently stronger. None of the EPS block samples tested reached a distinct maximum or ultimate shear stress.

165 The formation of two distinct phases in the shear stress-horizontal displacement diagram for the EPS block has  
166 also been reported by other researchers. The boundary between the two phases have been reported to form at 1 to  
167 4% strain depending on the density and dimensions of the geofoam, applied normal stress and the rate of loading  
168 [35, 37, 68]. This phenomenon is probably due to the fact that EPS particulates forming the geofoam block that are  
169 in contact with shear box walls become deformed and strained more than inner parts of the EPS block because of  
170 stress concentration. Hence, the deformed parts cannot fully contribute to increase in shear strength.

171 Figure 6 shows the relationship between maximum shear stress values reached at 7 mm displacement versus  
172 normal pressure for the 9 samples tested. Three failure envelopes have overlapped with the summary of the shear

173 strength parameters presented in Table 4. Results clearly show that for the EPS blocks apparent cohesion is the  
174 predominant parameter with an average value of 18 kPa with friction having very little influence on shear strength.  
175 The angles of internal friction determined have very low values of approximately  $3^\circ$ .

176 Summary of the direct shear tests conducted on EPS blocks by some other researchers are presented in Table 5.  
177 It observed that the shear strength parameters are influenced by factors such as normal stress, density and  
178 dimensions of EPS block. The smaller friction angle and the cohesion attained for EPS in current study is attributed  
179 to the lower density and the relatively larger normal stresses applied.

### 180 **3.2. Sand samples**

181 To determine sand's shear strength characteristics, a number of direct shear tests were performed on samples  
182 prepared at 60, 65, 70, 75, 80 and 100% relative densities. Figures 7 (a) to (f) show variations of shear stress-  
183 horizontal displacement for the above-mentioned specimens subjected to normal pressures of 100, 200 and 300 kPa.  
184 It is observed that at the low relative densities of 60 and 65%, shear stresses increase gradually with horizontal  
185 displacements and samples do not display distinct maximum or ultimate states. By increasing the relative densities  
186 to particularly 80 and 100%, shear stresses increase very rapidly with horizontal displacements and samples clearly  
187 show maximum and ultimate states which have overlapped. The rapid rates of increase in shear stresses signify  
188 stiffness and thus the higher the normal pressure, the greater the subsequent improvement in shear strengths. These  
189 changes in behavior are due to the greater confinements provided at higher normal pressures which restrict particle  
190 displacement and thus improve intergranular interactions [70, 71, 72, 73 & 74]. The differences in confinements and  
191 intergranular contact points in loose and dense sand is schematically shown in Fig. 8.

192 Figures 9 (a) to (f) portray vertical versus horizontal displacements for the sand samples having different relative  
193 densities. All samples show dilative behavior during shearing the amount of which substantially increases with the  
194 increase in density. The least and the most dilative changes have been displayed respectively by samples with  $R_d=60$   
195 and 100%. In samples with the lowest relative density of 60%, because of least intergranular interactions and the  
196 highest void ratio, particles do not effectively interact and easily slide past each other resulting in the lowest shear  
197 strength. In contrast in samples of higher relative densities, due to the presence of greater number of particles and  
198 lower void ratio in a constant volume, intergranular contacts significantly increase and grains cannot easily slide  
199 relative to each other during shearing and have to initially lift over adjacent particles and then displace. The lifting  
200 and the dislodgement of the soil grains result in increased void ratio and thus dilation. The amount of dilation  
201 reduces by increase in normal pressure which is attributed to probable particle breakage and the reduction in particle  
202 size. Also, the dilative behavior creates an uplift force, which is counteracted by the normal pressure which reduces  
203 the amount of dilation (see Fig. 10). Thus, the greater the normal pressure, the smaller the amount of dilation also  
204 confirmed by other researchers [75, 76, 77 & 78].

205 Failure envelopes for specimens with different relative densities are depicted in Figure 11, with summary of  
206 results presented in Table 6. Results are the average of two tests conducted on each particular sample which have  
207 been rounded to the nearest whole number. It is observed that by increasing the relative densities from 60 to 100%,

208 angles of internal friction have improved from 37 to 49 degrees and the apparent cohesions from 0 to 16 kPa  
209 representing enhancement in shear strength parameters of 32 and 160% respectively. It is worth mentioning that the  
210 apparent cohesions are attributed to inherent nature of direct shear apparatus and are small and thus can be neglected  
211 in designs.

### 212 **3.3. Sand-EPS particulate mixtures**

213 In the third stage of the investigation, direct shear tests were conducted on sand-EPS particulate mixtures. Sand  
214 was mixed with 0.1, 0.2 and 0.3% EPS particulates as dry weight of soil and compacted at relative densities of 60,  
215 65, 70, 75, 80 and 100%. To reduce the volume of the article, only the results of sand-EPS particulate mixtures with  
216 80% relative density have been presented in Figure 12. Results of equivalent sand samples without EPS particulates  
217 have also been included for comparative purposes. Results show that for samples subjected to a specific normal  
218 pressure, the inclusion of EPS particulates reduces shear stresses particularly with increase in normal pressure.  
219 Generally, samples containing higher percentage of EPS particulates, give lower shear stresses corresponding to a  
220 particular horizontal displacement and normal pressure. By the addition of EPS particulates of very low rigidity  
221 compared to sand particles, intergranular interactions and thus friction at interfaces is reduced leading to overall  
222 reduction of shear strength. EPS particulates have low density and high compressibility compared to soil particles.  
223 So, increasing the amount of EPS particulates in a constant volume, leads to the reduction of soil intergranular  
224 surfaces and thus overall reduction of shear strength. Results also show that with increase in normal pressure, the  
225 reduction in shear strength of the sand-EPS mixture increases. The increase in normal pressure causes compression  
226 of the highly compressible EPS particulates and thus reduces their interaction with sand grains leading to overall  
227 reduction in mixture shear strength. With increase in EPS content, not only sand-EPS particulate contact surfaces  
228 increase but also the probability of EPS-EPS particulate surfaces increases. These changes result in the reduction of  
229 sand-sand friction at interfaces which mainly contribute to shear strength clearly seen from the results depicted in  
230 Fig. 12.

231 Considering the behavior of sand-EPS particulate mixtures, the shear strengths attained could be the  
232 consequence of i) sand-sand, ii) sand-EPS, and iii) EPS-EPS interactions at contact surfaces also reported by Deng  
233 and Xiao, 2010 [29]. As sand particles have higher rigidity and strength in comparison with the EPS particulates, it  
234 would be logical to claim that their interactions (i.e. mechanism (i)) is the main contributor to the mixture shear  
235 strength and mechanisms (ii) and (iii) are less influential. Figure 12 clearly shows that regardless of the applied  
236 normal pressure, addition of EPS particulates to sand reduces the shear strength.

237 Figure 13 displays vertical versus horizontal displacements for sand-EPS particulate mixtures with  $R_d=80\%$   
238 subjected to  $\sigma_n=100, 200$  and  $300$  kPa. It is seen that all specimens show dilative behavior during shearing similar to  
239 sand samples. The amount of dilation demonstrates reduction with increase in normal pressures and EPS percentage.  
240 In specimen containing higher percentage of EPS particulates and exposed to greater normal pressures, soil grains  
241 penetrate the EPS particles preventing particle dislodgement and vertical displacement and subsequent rotation as a  
242 result of intergranular failure leading to overall reduction in dilation. At the same time greater normal pressures  
243 result in higher compression of the EPS particulates and thus further volume reduction. All sand-EPS mixtures

244 subjected to different normal pressures show smaller dilation at a particular horizontal displacement than sand  
245 samples clearly showing that EPS particulates restrict soil particle displacements.

246 The amount of dilation for sand and sand-EPS mixtures reduces with increase in normal pressure which is  
247 probably the result of some particle breakage at contact points in sand samples and the compression of the EPS  
248 particulates in sand-EPS mixtures. Probable sand-EPS interactions are schematically shown in Figure 14. As seen,  
249 with increase in EPS percentage, more sand particles can penetrate into EPS particulates. Therefore, the amount of  
250 the uplift force as well as the dilation of the sand-EPS mixture is further reduced. As mentioned earlier, normal  
251 pressure counteracts the uplift force, reducing its effect and the amount of dilation for reinforced and unreinforced  
252 sand. Different effects of higher compared to lower normal pressures on sand-EPS mixtures is that it allows sand  
253 particles to penetrate more into the EPS particulates both before and during shearing. In other words, higher normal  
254 pressure causes greater compression of the EPS particulates, which further reduces the dilation of the sand-EPS  
255 mixture.

256 Figure 15 demonstrates the relationship between maximum shear strengths and EPS content for mixtures with  
257  $R_d=80\%$ . It is observed that by the addition and increase in EPS content, maximum shear strengths reduce at all  
258 normal pressures examined and the rate of reduction increases with increase in the magnitude of normal pressure.  
259 Although EPS inclusion reduces maximum shear strengths, but it also reduces density of the soil-EPS mixture  
260 rendering it suitable for possible use as backfill for reduction of lateral pressure on earth retaining structures and  
261 save costs.

262 Variations of dilation angles with normal pressure for sand-EPS mixtures are shown in Figure 16. Results show  
263 that with increase in the magnitude of normal pressures as well as EPS content, dilation angles reduce. The  
264 relationship is approximately linear with the greatest rate of reduction displayed by sand-0.3% EPS particulate  
265 samples.

266 The influence of EPS particulates on shear strength parameters of the mixtures prepared with different densities  
267 are shown in Figures 17 and 18. Results show that in general by inclusion of EPS particulates, angle of internal  
268 friction reduces whereas apparent cohesions increase and at a particular EPS content, by increase in relative density,  
269 angles of internal friction are improved. This is caused by increase in the number of sand grains in the mixture  
270 promoting greater sand-sand intergranular interactions (i.e. mechanism (i)) as well as reduction in soil porosity  
271 resulting in higher friction and thus shear strengths. Presence of EPS particulates in mixtures reduce sand  
272 intergranular interactions resulting in the reduction of internal friction and thus shear strengths. In sand-0.1% EPS  
273 mixtures the angle of friction has increased by  $10^\circ$  whereas in sand-0.3% EPS specimens  $\phi$  has increased by  
274 approximately 8 degrees by increase in relative density from 60 to 80%. These changes distinctly show that at higher  
275 EPS contents, greater numbers of EPS particulates present result in the reduction of grain-grain interaction and  
276 subsequently the overall shear strength (Fig. 18).

277 Considering Figure 18, it is seen that by increase in relative density and subsequent reduction in void ratio,  
278 apparent cohesions in both sand and sand-EPS mixtures increase. Apparent cohesions in the sand samples may be  
279 attributed to the suction caused by the addition of small amount of water used for moistening the mixtures as well as



280 the internal mechanism of the direct shear apparatus. In accord with other researchers, it is suggested to neglect the  
281 low cohesion values [79 and 80]. For sand-EPS mixtures, as sand grains penetrate EPS particulates, their interaction  
282 using Mohr-Columb failure criteria appears as apparent cohesion also reported by Shirazi et al. (2018) [81]. With  
283 increase in relative density, the number of sand particles penetrating the EPS particulates increase, resulting in  
284 higher apparent cohesions.

285 By increasing relative density of mixtures, the shear strengths and therefore bearing capacity is improved. As a  
286 result of compaction for achieving the desired densities, sand grains and EPS particulates become tightly  
287 compressed and consequently void ratio reduces resulting in greater and more effective interactions at interfaces.  
288 Improved interactions increase stiffness and therefore shear strength of the mixtures. According to the results shown  
289 on Figure 19, the highest shear strength of 320 kPa was achieved by sand+0.1% EPS mixture with  $R_d=80\%$   
290 subjected to  $\sigma_n=300$  kPa and the lowest shear strength of 75.4 kPa was attained by samples of sand+0.2%EPS  
291 particulates with  $R_d=60\%$  at  $\sigma_n=100$  kPa. Reduction in shear strength of samples with the highest relative density of  
292 80% and 0.3% EPS particulate subjected to normal pressures of 300 kPa is greater than the specimens with lowest  
293 relative density of 60% subjected to  $\sigma_n=100$  kPa. This is attributed to the greater number of EPS particulates in a  
294 constant volume resulting in the reduction of sand intergranular interactions.

295 Dense granular materials tend to dilate whereas loose granular materials show compression during shearing.  
296 Dilation angle ( $\Psi$ ) is determined by the equation 1 using the values of vertical and horizontal displacements that  
297 represent maximum slope of the vertical versus horizontal displacement curves.

$$298 \quad \tan(\Psi) = \frac{dv}{dh}$$

299 (1)

300 Figure 20 presents the effects of EPS content and normal pressure on dilation angles at different relative  
301 densities. The highest dilation angle of  $20.7^\circ$  was achieved by the sand+0.1% EPS mixture with relative density of  
302 80% and subjected to normal pressure of 100 kPa. By increasing relative density, vertical stress and EPS content in  
303 mixtures, dilatation angles decrease due to compressibility of EPS particles and thus overall reduction in volume  
304 changes.

#### 305 **4. Conclusions**

306 The use of lightweight backfills behind earth retaining structures can significantly reduce lateral pressures or  
307 alleviate seismic forces. One of the methods is to use EPS blocks behind retaining structures which in irregular  
308 conditions is rather difficult and thus can be replaced by EPS particulates which can easily be mixed with soil in just  
309 the same manner as chemical admixtures. In current study the effects of EPS particulates on shear strength  
310 characteristics of sand with different relative densities and subjected to various normal pressures has been  
311 investigated and the following conclusions reached:

- 312 • Increasing the relative density, significantly improves shear strength characteristics of sand and by the inclusion  
313 of EPS particulates, shear strength characteristics of the mixtures are reduced. EPS particulate addition to sand  
314 reduces the angle of internal friction and increases apparent cohesion of mixtures.
- 315 • The addition of EPS particulates reduces the dry unit weight of mixtures which have the potential to be used as  
316 light weight backfill in geotechnical engineering projects. Due to the high compressible potential of the EPS  
317 particulates, increasing normal pressure significantly reduces dilation of mixtures. The higher the normal  
318 pressure, the lower the dilation of mixture.
- 319 • By increasing the relative density of the samples, the shear strength characteristics of mixtures increase due to  
320 the decrease in porosity and the more effective intergranular interactions. Also, as the relative density of  
321 mixtures increase, the amount of dilation and the dilation angles increase. By increasing the relative density,  
322 mixtures become and behave more rigidly and reach failure state at lower shear displacements.
- 323 • By increasing the relative densities from 60 to 100%, angles of internal friction improved from 37 to 49 degrees  
324 and the apparent cohesions from 0 to 16 kPa which represent enhancement in shear strength parameters of 32  
325 and 160% respectively.
- 326 • According to the important results of this study, the inclusion of EPS particulates in sand does not result in a  
327 significant reduction in shear strength. Therefore, EPS can be used in various construction projects as blocks or  
328 particulates in combination with soil. It can be used for railways, slope stability, backfill in retaining structures,  
329 and fill in embankments.

## 330 **5. Data Availability Statement**

331 All data, models or code that support the findings of the current study are available from the corresponding  
332 author upon reasonable request.

## 333 **6. Declaration of interests**

334 The authors declare that they have no known competing financial interests or personal relationships that could  
335 have appeared to influence the work reported in this paper.

## 336 **7. References**

- 337 [1] Horvath, J. S. “The compressible inclusion function of EPS geof foam”, *Geotextiles and Geomembranes*, **15**(1-3),  
338 pp. 77-120 (1997). [https://doi.org/10.1016/S0266-1144\(97\)00008-3](https://doi.org/10.1016/S0266-1144(97)00008-3)
- 339 [2] Shukla, S. K., and Yin, J. H. “Fundamentals of geosynthetic engineering”, CRC Press, London, UK (2006).
- 340 [3] Han, J. “Principles and practice of ground improvement”, John Wiley & Sons, Hoboken, New Jersey, USA  
341 (2015).
- 342 [4] Tiwari, N., Satyam, N., and Shukla, S. K. “An experimental study on micro-structural and geotechnical  
343 characteristics of expansive clay mixed with EPS granules”, *Soils and Foundations*, **60**(3), pp. 705-713 (2020).  
344 <https://doi.org/10.1016/j.sandf.2020.03.012>

345 [5] Shu, Y. H., Zhang, J. S., Fang, A. N., et al. "Effect of coupled chloride salt erosion and Freeze-thaw on the  
346 dynamic mechanical properties of EPS cement soils", *Construction and Building Materials*, **375**, 130951 (2023).  
347 <https://doi.org/10.1016/j.conbuildmat.2023.130951>

348 [6] Jiang, P., Zheng, W., Zhou, et al. "Laboratory characterization of soft clay mixed with EPS, lime, fly ash, and  
349 sodium silicate", *Bulletin of Engineering Geology and the Environment*, **82**(8), 302, pp. 1-14 (2023).  
350 <https://doi.org/10.1007/s10064-023-03297-y>

351 [7] Hatami, K., and Witthoef, A. F. "A numerical study on the use of geof foam to increase the external stability of  
352 reinforced soil walls", *Geosynthetics International*, **15**(6), pp. 452-470 (2008).  
353 <https://doi.org/10.1680/gein.2008.15.6.452>

354 [8] Ertugrul, O. L., and Trandafir, A. C. "Reduction of lateral earth forces acting on rigid nonyielding retaining walls  
355 by EPS geof foam inclusions", *Journal of Materials in Civil Engineering*, **23**(12), pp. 1711-1718. (2011).  
356 [https://doi.org/10.1061/\(ASCE\)MT.1943-5533.0000348](https://doi.org/10.1061/(ASCE)MT.1943-5533.0000348)

357 [9] Ossa, A., and Romo, M. P. "Dynamic characterization of EPS geof foam", *Geotextiles and Geomembranes*, **29**(1),  
358 pp. 40-50 (2011). <https://doi.org/10.1016/j.geotextmem.2010.06.007>

359 [10] Bartlett, S. F., Lingwall, B. N., and Vaslestad, J. "Methods of protecting buried pipelines and culverts in  
360 transportation infrastructure using EPS geof foam", *Geotextiles and Geomembranes*, **43**(5), pp. 450-461 (2015).  
361 <https://doi.org/10.1016/j.geotextmem.2015.04.019>

362 [11] Beju, Y. Z., and Mandal, J. N. "Combined use of jute geotextile-EPS geof foam to protect flexible buried pipes:  
363 Experimental and numerical studies", *International Journal of Geosynthetics and Ground Engineering*, **3**(4), pp. 1-  
364 20 (2017). <https://doi.org/10.1007/s40891-017-0107-5>

365 [12] Meguid, M. A., and Hussein, M. O. G. "A numerical procedure for the assessment of contact pressures on  
366 buried structures overlain by EPS geof foam inclusion", *International Journal of Geosynthetics and Ground  
367 Engineering*, **3**(1), pp. 1-14 (2017). <https://doi.org/10.1007/s40891-016-0078-y>

368 [13] AbdelSalam, S.S., Anwar, M.B., and Eskander, S.S. (2019). "Long Term Behavior of EPS Geof foam for Road  
369 Embankments", *2nd GeoMEast International Congress and Exhibition Sustainable Civil Infrastructure*, Egypt, pp.  
370 97-107 (2018). [https://doi.org/10.1007/978-3-030-01944-0\\_8](https://doi.org/10.1007/978-3-030-01944-0_8)

371 [14] Ghotbi Siabil, S. M. A., Moghaddas Tafreshi, S. N., Dawson, A. R., et al. "Behavior of expanded polystyrene  
372 (EPS) blocks under cyclic pavement foundation loading", *Geosynthetics International*, **26**(1), pp. 1-25 (2019).  
373 <https://doi.org/10.1680/jgein.18.00033>

374 [15] Meguid, M. A., and Ahmed, M. R. "Earth pressure distribution on buried pipes installed with geof foam  
375 inclusion and subjected to cyclic loading", *International Journal of Geosynthetics and Ground Engineering*, **6**(1),  
376 pp. 1-8 (2020). <https://doi.org/10.1007/s40891-020-0187-5>

377 [16] Puppala, A. J., Banerjee, A., and Congress, S. S. “Geosynthetics in geo-infrastructure applications”,  
378 In *Durability of Composite Systems*, K. L. Reifsnider, Ed., pp. 289-312. Woodhead Publishing, Duxford, UK (2020).  
379 <https://doi.org/10.1016/B978-0-12-818260-4.00007-7>

380 [17] Sarkar, A., Barman, R., and Bhowmik, D. “Numerical Investigation on Vibration Screening Using Geofoam  
381 and Sand–Crumb Rubber Mixture Infilled Trench”, *International Journal of Geosynthetics and Ground*  
382 *Engineering*, **7**(4), pp. 1-14 (2021) <https://doi.org/10.1007/s40891-021-00329-z>

383 [18] Malai, A., and Youwai, S. “Stiffness of expanded polystyrene foam for different stress states”, *International*  
384 *Journal of Geosynthetics and Ground Engineering*, **7**(4), pp. 1-11 (2021). [https://doi.org/10.1007/s40891-021-](https://doi.org/10.1007/s40891-021-00321-7)  
385 [00321-7](https://doi.org/10.1007/s40891-021-00321-7)

386 [19] Khan, M. I., and Meguid, M. A. “A Numerical Study on the Role of EPS Geofoam in Reducing Earth Pressure  
387 on Retaining Structures Under Dynamic Loading”, *International Journal of Geosynthetics and Ground*  
388 *Engineering*, **7**(3), pp. 1-14 (2021). <https://doi.org/10.1007/s40891-021-00304-8>

389 [20] Ge, Q., Zuo, W., Liu, R., et al. “Experimental Studies for Shear and Multi-Impact Resistance Performance of  
390 Sand–Geofoam Material”, *Buildings*, **12**(5), 633, pp. 1-18 (2022). <https://doi.org/10.3390/buildings12050633>

391 [21] Duan, C., and Zheng, M. “Application of EPS to Mitigate Ground Movements Caused by Mechanized  
392 Tunneling”, *Geotechnical and Geological Engineering*, pp. 1-17 (2023). [https://doi.org/10.1007/s10706-023-](https://doi.org/10.1007/s10706-023-02642-y)  
393 [02642-y](https://doi.org/10.1007/s10706-023-02642-y)

394 [22] Yang, X. “Performance of Geofoam Included Nailed-Walls in Dynamic Condition”, *Geotechnical and*  
395 *Geological Engineering*, pp. 1-16 (2023). <https://doi.org/10.1007/s10706-023-02656-6>

396 [23] Miki, G. “Ten Year History of EPS Method in Japan and Its Future Challenges”, *International Symposium on*  
397 *EPS Construction Method*, Tokyo, Japan: pp. 394-411 (1996).

398 [24] Negussey, D. “Properties and applications of geofoam, society of the plastics industry”, *Society of the Plastics*  
399 *Industry*, Washington, USA (1997).

400 [25] Chrysikos, D., Atmatzidis, D., and Missirlis, E. “EPS geofoam surface shear resistance”, *8th IGS, Yokohama,*  
401 *Japan*, pp. 1647-1650 (2006).

402 [26] Liu, H. L., Deng, A., and Chu, J. “Effect of different mixing ratios of polystyrene pre-puff beads and cement on  
403 the mechanical behaviour of lightweight fill”, *Geotextiles and Geomembranes*, **24**(6), pp. 331-338 (2006).  
404 <https://doi.org/10.1016/j.geotexmem.2006.05.002>

405 [27] Abdelrahman, G. E., Duttine, A., and Tatsuoka, F. “Interface friction properties of EPS geofoam blocks from  
406 direct shear tests”, *Symposium on Characterization and Behavior of Interfaces*, Atlanta, Georgia, USA, pp. 113-118  
407 (2008).

408 [28] Kim, Y. T., Kim, H. J., and Lee, G. H. “Mechanical behavior of lightweight soil reinforced with waste fishing  
409 net”, *Geotextiles and Geomembranes*, **26**(6), pp. 512-518 (2008). <https://doi.org/10.1016/j.geotexmem.2008.05.004>

- 410 [29] Deng, A., and Xiao, Y. “Measuring and modeling proportion-dependent stress-strain behavior of EPS-sand  
411 mixture. American Society of Civil Engineers”, *International Journal of Geomechanics*, **10**(6), pp. 214-222 (2010).  
412 [https://doi.org/10.1061/\(ASCE\)GM.1943-5622.0000062](https://doi.org/10.1061/(ASCE)GM.1943-5622.0000062)
- 413 [30] Heydarian, H., Nejad Shirazi, A., and Nasehi, A. “Study of Geofoam Weight Percent Effects on Bearing  
414 Capacity of Lighted Soil by Geofoam”, *First National Conference on Civil Engineering*, Zibakenar, Iran, pp. 1-6  
415 (2012). (In Persian)
- 416 [31] Rocco, N. T., and Luna, R., “Mixtures of clay/EPS particulates and undrained shear strength”, In *Geo-*  
417 *Congress: Stability and Performance of Slopes and Embankments III*, San Diego, California, United States, pp.  
418 2059-2068 (2013). <https://doi.org/10.1061/9780784412787.208>
- 419 [32] Padade, A. H., and Mandal, J. N. “Expanded polystyrene-based geomaterial with fly ash”, *International*  
420 *Journal of Geomechanics*, **14**(6), pp. 1-7 (2014). [https://doi.org/10.1061/\(ASCE\)GM.1943-5622.0000390](https://doi.org/10.1061/(ASCE)GM.1943-5622.0000390)
- 421 [33] Edinçliler, A., and Özer, A. T. “Effects of EPS bead inclusions on stress–strain behaviour of  
422 sand”, *Geosynthetics International*, **21**(2), pp. 89-102 (2014). <https://doi.org/10.1680/gein.14.00001>
- 423 [34] Padade, A. H., and Mandal, J. N. “Interface strength behavior of expanded polystyrene EPS  
424 geofoam”, *International Journal of Geotechnical Engineering*, **8**(1), 66-71 (2014).  
425 <https://doi.org/10.1179/1938636213Z.00000000056>
- 426 [35] Özer, A. T., and Akay, O. “Interface shear strength characteristics of interlocked EPS-block geofoam”, *Journal*  
427 *of Materials in Civil Engineering*, **28**(4), 04015156, pp. 1-13. (2016). [https://doi.org/10.1061/\(ASCE\)MT.1943-5533.0001418](https://doi.org/10.1061/(ASCE)MT.1943-5533.0001418)
- 429 [36] AbdelSalam, S. S., and Azzam, S. A. “Reduction of lateral pressures on retaining walls using geofoam  
430 inclusion”, *Geosynthetics International*, **23**(6), pp. 395-407 (2016). <https://doi.org/10.1680/jgein.16.00005>
- 431 [37] Khan, M. I., and Meguid, M. A. “Experimental investigation of the shear behavior of EPS  
432 geofoam”, *International Journal of Geosynthetics and Ground Engineering*, **4**(2), pp. 1-12 (2018).  
433 <https://doi.org/10.1007/s40891-018-0129-7>
- 434 [38] El-Sherbiny, R. M., Ramadan, S. H., and El-Khouly, M. A. “Dynamic properties of sand-EPS bead  
435 mixtures”, *Geosynthetics International*, **25**(4), pp. 456-470 (2018). <https://doi.org/10.1680/jgein.18.00021>
- 436 [39] Alaie, R., and Jamshidi Chenari, R. “Cyclic and post-cyclic shear behaviour of interface between geogrid and  
437 EPS beads-sand backfill”, *KSCE Journal of Civil Engineering*, **22**(9), pp. 3340-3357 (2018).  
438 <https://doi.org/10.1007/s12205-018-0945-2>
- 439 [40] Alaie, R., and Jamshidi Chenari, R. “Dynamic properties of EPS-sand mixtures using cyclic triaxial and bender  
440 element tests”, *Geosynthetics International*, **26**(6), pp. 563-579 (2019). <https://doi.org/10.1680/jgein.19.00034>

- 441 [41] Jamshidi Chenari, R., Ebrahimi Khonachah, R., Hosseinpour, I., et al. “An experimental study for the cyclic  
442 interface properties of the EPS–sand mixtures reinforced with geogrid”, *International Journal of Civil*  
443 *Engineering*, **18**(2), pp. 151-159 (2020). <https://doi.org/10.1007/s40999-019-00424-3>
- 444 [42] Nawghare, S. M., and Mandal, J. N. “Effectiveness of expanded polystyrene (EPS) beads size on fly ash  
445 properties”, *International Journal of Geosynthetics and Ground Engineering*, **6**(1), pp. 1-11 (2020).  
446 <https://doi.org/10.1007/s40891-020-0189-3>
- 447 [43] Ali, S., Yong, F., Marri, A., et al. “Effect of expanded polystyrene beads and fly ash on the strength and  
448 deformation characteristics of soil”, *Journal of Xi’an Shiyou University, Natural Science Edition*, **19**(2), pp. 829-841  
449 (2023). <https://www.xisdjxsu.asia/V19I02-71.pdf>
- 450 [44] Abbasimaedeh, P., Ghanbari, A., O’Kelly, B. C., et al. “Geomechanical behaviour of uncemented expanded  
451 polystyrene (EPS) beads–clayey soil mixtures as lightweight fill”, *Geotechnics*, **1**(1), pp. 38-58 (2021).  
452 <https://doi.org/10.3390/geotechnics1010003>
- 453 [45] Alaie, R., Jamshidi Chenari, R., & Karimpour-Fard, M. “Shaking table study on sand-EPS beads-mixtures  
454 using a laminar box”, *Geosynthetics International*, **28**(3), pp. 224-237 (2021).  
455 <https://doi.org/10.1680/jgein.20.00039>
- 456 [46] Zhu, L., Wen, K., Tong, R., et al. “Dynamic Shear Strength Characteristics of Lightweight Sand-EPS  
457 Soil”, *Sustainability*, **14**(12), pp. 1-9 (2022). <https://doi.org/10.3390/su14127397>
- 458 [47] Ge, Q., Zuo, W., Liu, R., et al. “Experimental studies for shear and multi-impact resistance performance of sand  
459 geofom material”, *Buildings*, **12**(5), pp. 1-18 (2022). <https://doi.org/10.3390/buildings12050633>
- 460 [48] Jili, Q., Huan, T., Weiqing, Q., et al. “Modification of mechanical properties of Shanghai clayey soil with  
461 expanded polystyrene”, *Science and Engineering of Composite Materials*, **29**(1), pp. 37-46 (2022).  
462 <https://doi.org/10.1515/secm-2022-0004>
- 463 [49] Bekranbehesht, B., Rezvani, R., Payan, M., et al. “Nondestructive Shear Stiffness Evaluation of EPS-Sand  
464 Composites Using Quartz and Calcareous Aggregates”, *Journal of Materials in Civil Engineering*, **35**(7), 04023174,  
465 pp. 1-18 (2023). <https://doi.org/10.1061/JMCEE7.MTENG-151>
- 466 [50] Tao, H., Zheng, W., Zhou, X., et al. “Study on Dynamic Modulus and Damping Characteristics of Modified  
467 Expanded Polystyrene Lightweight Soil under Cyclic Load”, *Polymers*, **15**(8), 1865, pp. 1-17 (2023).  
468 <https://doi.org/10.3390/polym15081865>
- 469 [51] Karimpour-Fard, M., Ashouryan, E., Rezaie Soufi, G., et al. “Experimental review on the effective stress  
470 equation in sand–EPS mixtures”, *Geomechanics and Geoengineering*, **18**(5), pp. 380-393 (2023).  
471 <https://doi.org/10.1080/17486025.2022.2056642>
- 472 [52] Demiröz, A., and Diker, Ö. “Investigation of the geotechnical properties of lightweight fill ground containing  
473 EPS-waste tire”, *Advanced Engineering Science*, **3**, pp. 112-124 (2023).  
474 <https://publish.mersin.edu.tr/index.php/ades/article/view/1053>

- 475 [53] Karademir, T. “Counterface soil type and loading condition effects on granular/cohesive soil–Geofoam  
476 interface shear behavior”, *Turkish Journal of Engineering*, **8**(1), pp. 76-91 (2023).  
477 <https://doi.org/10.31127/tuje.1279304>
- 478 [54] Hatami, K., Esmaili, D., Chan, E. C., et al. “Laboratory performance of reduced-scale reinforced embankments  
479 at different moisture contents”, *International Journal of Geotechnical Engineering*, **8**(3), pp. 260-276 (2014).  
480 <https://doi.org/10.1179/1939787914Y.0000000051>
- 481 [55] Hatami, K., Esmaili, D., Chan, E. C., et al. “Moisture reduction factors for shear strength of unsaturated  
482 reinforced embankments”, *International Journal of Geomechanics*, **16**(6), D4016001, pp. 1-16 (2016).  
483 [https://doi.org/10.1061/\(ASCE\)GM.1943-5622.0000624](https://doi.org/10.1061/(ASCE)GM.1943-5622.0000624)
- 484 [56] Abdi, M. R., Zandieh, A. R., Mirzaeifar, H., et al. “Influence of geogrid type and coarse grain size on pull out  
485 behaviour of clays reinforced with geogrids embedded in thin granular layers”, *European Journal of Environmental  
486 and Civil Engineering*, **25**(12), pp. 2161-2180 (2019). <https://doi.org/10.1080/19648189.2019.1619627>
- 487 [57] Abdi, M. R., Nakhaei, P., and Safdari Seh Gonbad, M. “Prediction of enhanced soil–anchored geogrid  
488 interactions in direct shear mode using gene expression programming”, *Geotechnical and Geological  
489 Engineering*, **39**, pp. 957-972 (2021). <https://doi.org/10.1007/s10706-020-01537-6>
- 490 [58] Mirzaeifar, H., Hatami, K., and Abdi, M. R. “Pullout testing and Particle Image Velocimetry (PIV) analysis of  
491 geogrid reinforcement embedded in granular drainage layers”, *Geotextiles and Geomembranes*, **50**(6), pp. 1083-  
492 1109 (2022). <https://doi.org/10.1016/j.geotexmem.2022.06.008>
- 493 [59] Abdi, M. R., Mirzaeifar, H., and Asgardun, Y. “Novel soil-pegged geogrid (PG) interactions in pull-out loading  
494 conditions”, *Geotextiles and Geomembranes*, **50**(4), pp. 764-778 (2022).  
495 <https://doi.org/10.1016/j.geotexmem.2022.04.001>
- 496 [60] Abdi, M. R., Tabarsa, A., and Haghgouy, P. “Evaluation of Soil–Geometrically Modified Geogrid Interaction  
497 in Direct Shear Mode”, *International Journal of Geosynthetics and Ground Engineering*, **9**(5), 60, pp. 1-16 (2023).  
498 <https://doi.org/10.1007/s40891-023-00479-2>
- 499 [61] Abdi, M. R., Mirzaeifar, H., Asgardun, Y., et al. “Assessment of pegged geogrid (PG) pullout performance in  
500 coarse-grained soils using PIV analysis”, *Geotextiles and Geomembranes*. **52**(1), pp. 27-45 (2023).  
501 <https://doi.org/10.1016/j.geotexmem.2023.09.001>
- 502 [62] ASTM D4253-16. “Standard Test Methods for Maximum Index Density and Unit Weight of Soils Using a  
503 Vibratory Table”, *ASTM International*, West Conshohocken (2016). DOI: [10.1520/D4253-16](https://doi.org/10.1520/D4253-16)
- 504 [63] ASTM D4254-16. “Standard Test Methods for Minimum Index Density and Unit Weight of Soils and  
505 Calculation of Relative Density”, *ASTM International*, West Conshohocken (2016). DOI: [10.1520/D4254-16](https://doi.org/10.1520/D4254-16)
- 506 [64] ASTM D6913/D6913M-17. “Standard Test Methods for Particle-Size Distribution (Gradation) of Soils Using  
507 Sieve Analysis”, *ASTM International*, West Conshohocken (2017). DOI: [10.1520/D6913-17](https://doi.org/10.1520/D6913-17)
- 508 [65] ASTM D422-63. “Standard Test Method for Particle-Size Analysis of Soils”, *ASTM International*, West  
509 Conshohocken (2007).

510 [66] ASTM D6817/D6817M-17. “Standard Specification for Rigid Cellular Polystyrene Geofoam”, *ASTM*  
511 *International*, West Conshohocken (2021). [DOI: 10.1520/D6817\\_D6817M-17R21](https://doi.org/10.1520/D6817_D6817M-17R21)

512 [67] ASTM D3080-04. “Standard Test Method for Direct Shear Test of Soils Under Consolidated Drained  
513 Conditions”, *ASTM International*, West Conshohocken (2004). [DOI: 10.1520/D3080-04](https://doi.org/10.1520/D3080-04)

514 [68] Meguid, M. A., and Khan, M. I. “On the role of geofoam density on the interface shear behavior of composite  
515 geosystems”, *International Journal of Geo-Engineering*, **10**(1), pp. 1-18 (2019). [https://doi.org/10.1186/s40703-](https://doi.org/10.1186/s40703-019-0103-9)  
516 [019-0103-9](https://doi.org/10.1186/s40703-019-0103-9)

517 [69] Padade, A. H., and Mandal, J. N. “Direct shear test on expanded polystyrene (EPS) geofoam”, *5th European*  
518 *Geosynthetic Congress, International Geosynthetics Society*, Valencia, Spain, pp. 1-4 (2012).

519 [70] Sivathayalan, S., and Ha, D. “Effect of static shear stress on the cyclic resistance of sands in simple shear  
520 loading”, *Canadian Geotechnical Journal*, **48**(10), pp. 1471-1484 (2011). <https://doi.org/10.1139/t11-05>

521 [71] Omidvar, M., Iskander, M., and Bless, S. “Stress-strain behavior of sand at high strain rates”, *International*  
522 *journal of impact engineering*, **49**, pp. 192-213 (2012). <https://doi.org/10.1016/j.ijimpeng.2012.03.004>

523 [72] Abdi, M. R., and Safdari Seh Gonbad, M. “Enhancement of soil-geogrid interactions in direct shear mode using  
524 attached elements as anchors”, *European Journal of Environmental and Civil Engineering*, **24**(8), pp. 1161-1179  
525 (2018). <https://doi.org/10.1080/19648189.2018.1454861>

526 [73] Abdi, M. R., and Safdari Seh Gonbad, M. “Studying the effect of roughness on soil-geotextile interaction in  
527 direct shear test”, *Journal of Engineering Geology*, **12**(5), pp. 1-30 (2018). <http://jeg.khu.ac.ir/article-1-2733-en.html>

528 [74] Abdi, M. R., and Rashed, H. “Shear Strength Enhancement Prediction of Sand–Fiber Mixtures Using Genetic  
529 Expression Programming”, *Journal of Materials in Civil Engineering*, **33**(11), 04021323, pp. 1-14 (2021).  
530 [https://doi.org/10.1061/\(ASCE\)MT.1943-5533.0003954](https://doi.org/10.1061/(ASCE)MT.1943-5533.0003954)

531 [75] Bolton, M. D. “The strength and dilatancy of sands”, *Geotechnique*, **36**(1), pp. 65-78 (1986).  
532 <https://doi.org/10.1680/geot.1986.36.1.65>

533 [76] Dove, J. E., and Jarrett, J. B. “Behavior of dilative sand interfaces in a geotribology framework”, *Journal of*  
534 *Geotechnical and Geoenvironmental Engineering*, **128**(1), 25-37 (2002). [https://doi.org/10.1061/\(ASCE\)1090-](https://doi.org/10.1061/(ASCE)1090-0241(2002)128:1(25))  
535 [0241\(2002\)128:1\(25\)](https://doi.org/10.1061/(ASCE)1090-0241(2002)128:1(25))

536 [77] Tuna, S. C., and Altun, S. “Mechanical behaviour of sand-geotextile interface”, *Scientia Iranica*, **19**(4), pp.  
537 1044-1051 (2012). <https://doi.org/10.1016/j.scient.2012.06.009>

538 [78] Abdi, M. R., and Hossienabadi, A. “Optimizing the Microanchor Attachment Angle for Maximum Interaction  
539 Enhancement at Granular Soils-Geogrid Interface under Direct Shear Mode”, *International Journal of*  
540 *Geomechanics*, **23**(4), 04023025, pp. 1-12 (2023). <https://doi.org/10.1061/IJGNALGMENG-7906>



541 [79] Abdi, M. R., Sadrnejad, A., and Arjomand, M. A. "Strength enhancement of clay by encapsulating geogrids in  
542 thin layers of sand", *Geotextiles and Geomembranes*, **27**(6), pp. 447-455 (2009).  
543 <https://doi.org/10.1016/j.geotexmem.2009.06.001>

544 [80] Abdi, M. R., Sadrnejad, S. A., and Arjomand, M. A. "Clay reinforcement using geogrid embedded in thin  
545 layers of sand", *International Journal of Civil Engineering*, **7**(4), pp. 224-235 (2009). <http://ijce.iust.ac.ir/article-1-380-en.html>  
546

547 [81] Nejad Shirazi, A., Haydarian, H., & Nasehi, S. A. "Shear and compression behaviors of sandy and clayey soils  
548 mixed with different sizes of expanded polystyrene beads", *Geotechnical and Geological Engineering*, **36**(6), 3823-  
549 3830 (2018). <https://doi.org/10.1007/s10706-018-0575-y>

550

551

552 **Figures captions:**

553 **Figure 1.** Sand particle size distribution curve.

554 **Figure 2.** EPS particulates.

555 **Figure 3.** Schematic of direct shear test apparatus.

556 **Figure 4.** Illustration of samples prepared for direct shear testing: a) sand-EPS particulate mixture and b) EPS block.

557 **Figure 5.** Shear stress-horizontal displacement of EPS block.

558 **Figure 6.** Failure envelopes for EPS blocks.

559 **Figure 7.** Shear stress-horizontal displacement of sand at: a) 60%, b) 65%, c) 70%, d) 75%, e) 80% and f) 100%  
560 relative densities.

561 **Figure 8.** Comparison of intergranular points and confinements in direct shear test: a) idealized loose and b) dense  
562 sand.

563 **Figure 9.** Vertical versus horizontal displacements of sands at: a) 60%, b) 65%, c) 70%, d) 75%, e) 80% and f)  
564 100% relative densities.

565 **Figure 10.** Interaction of normal pressure and uplift forces on sand grains during shearing.

566 **Figure 11.** Failure envelopes for sands with different relative densities.

567 **Figure 12.** Shear stress-horizontal displacement of sand-EPS particulate mixtures with  $R_d=80\%$ ; a)  $\sigma_n=100$  kPa, b)  
568  $\sigma_n=200$  kPa, c)  $\sigma_n=300$  kPa.

569 **Figure 13.** Vertical-Horizontal Displacement of sand-EPS mixtures with  $R_d=80\%$ ; a)  $\sigma_n=100$  kPa, b)  $\sigma_n=200$  kPa,  
570 c)  $\sigma_n=300$  kPa.

571 **Figure 14.** Position of sand and EPS particles before and after shearing.

572 **Figure 15.** Variations of maximum shear strength-EPS content in mixtures with  $R_d=80\%$ .

573 **Figure 16.** Dilation angle-normal pressure for sand-EPS mixtures with  $R_d=80\%$ .

574 **Figure 17.** Friction angle-EPS content in mixtures with different relative densities.

575 **Figure 18.** Apparent cohesion-EPS content in mixtures with different relative densities.

576 **Figure 19.** Shear Strength-EPS content of all mixtures.

577 **Figure 20.** Variations of dilation angles for sand-EPS mixtures of different densities subjected to  $\sigma_n=100, 200$  and  
578 300 kPa.

579

580 **Tables' captions:**

581 **Table 1.** Sand characteristics

582 **Table 2.** Physical and mechanical properties of EPS particulates

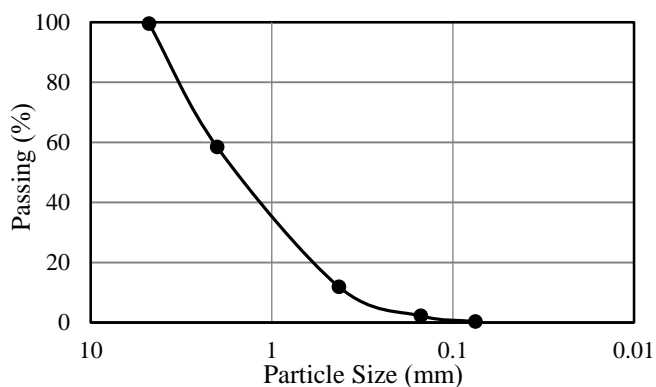
583 **Table 3.** Sand-EPS particulate mixtures investigated

584 **Table 4.** Shear strength parameter for EPS blocks

585 **Table 5.** Summary of direct shear test conducted on EPS blocks

586 **Table 6.** Summary of sand shear strength parameters at different relative densities

587 **Figures:**



588

589 **Figure 1.** Sand particle size distribution curve.

590

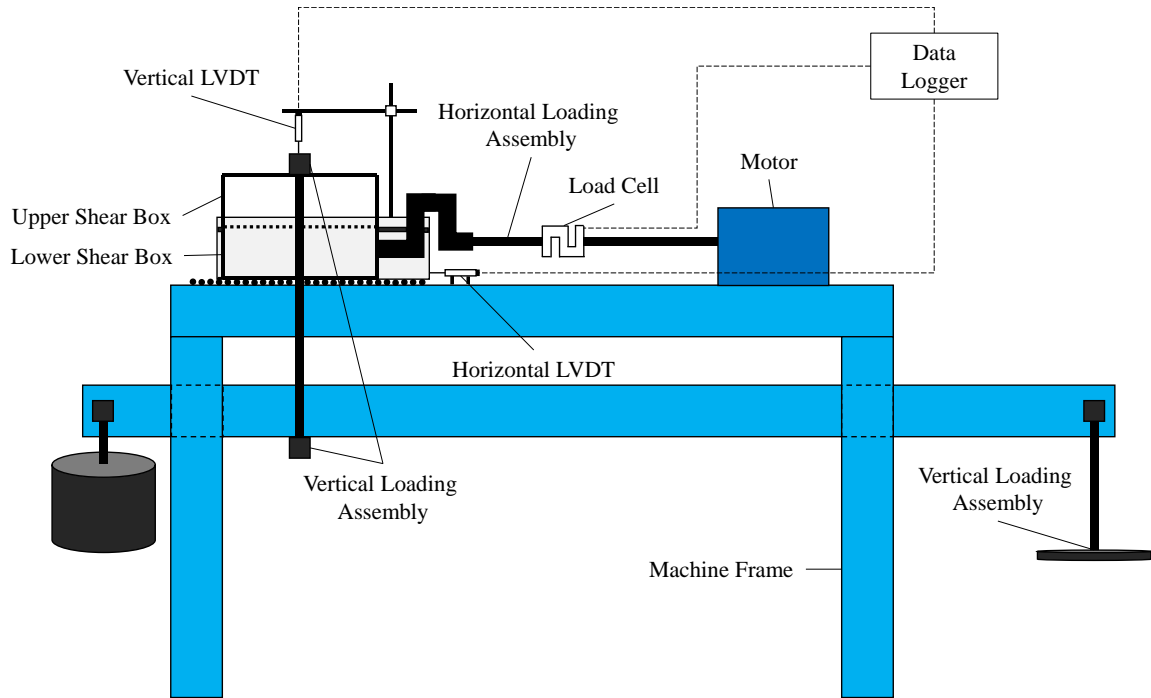
591



592

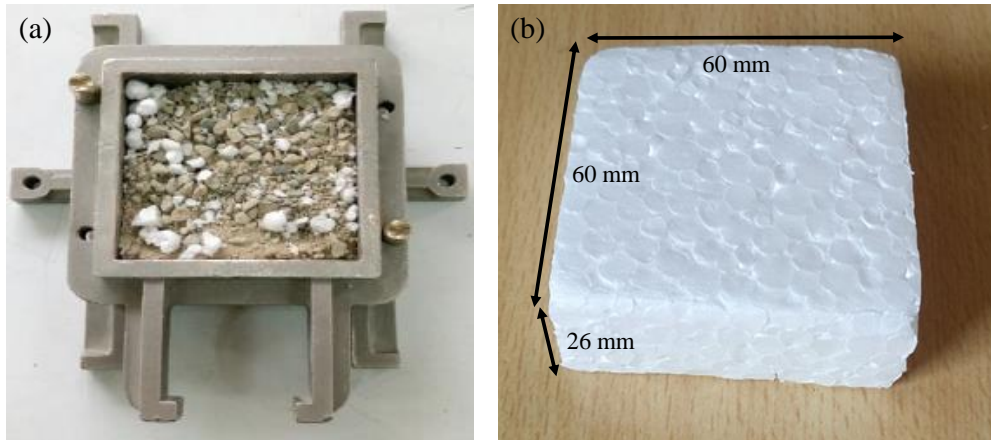
593 **Figure 2.** EPS particulates.

594

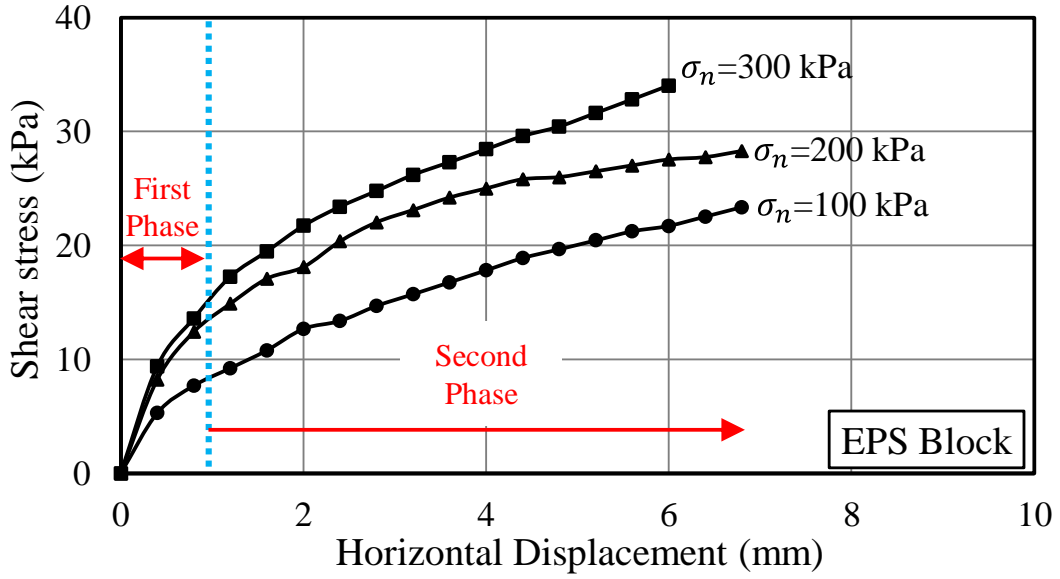


595  
596 **Figure 3.** Schematic of direct shear test apparatus.  
597

598  
599

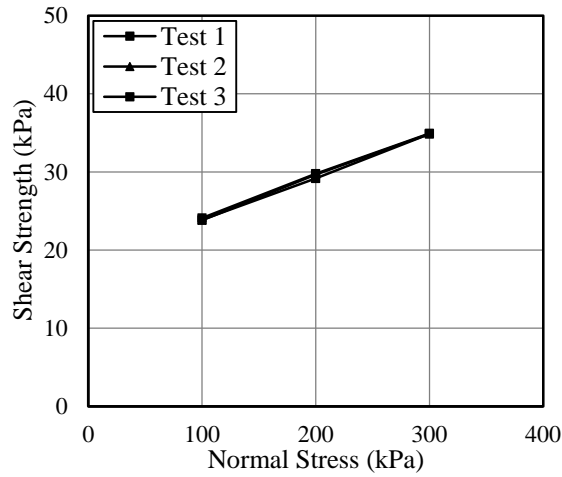


600 **Figure 4.** Illustration of samples prepared for direct shear testing: a) sand-EPS particulate mixture and b) EPS block.  
601



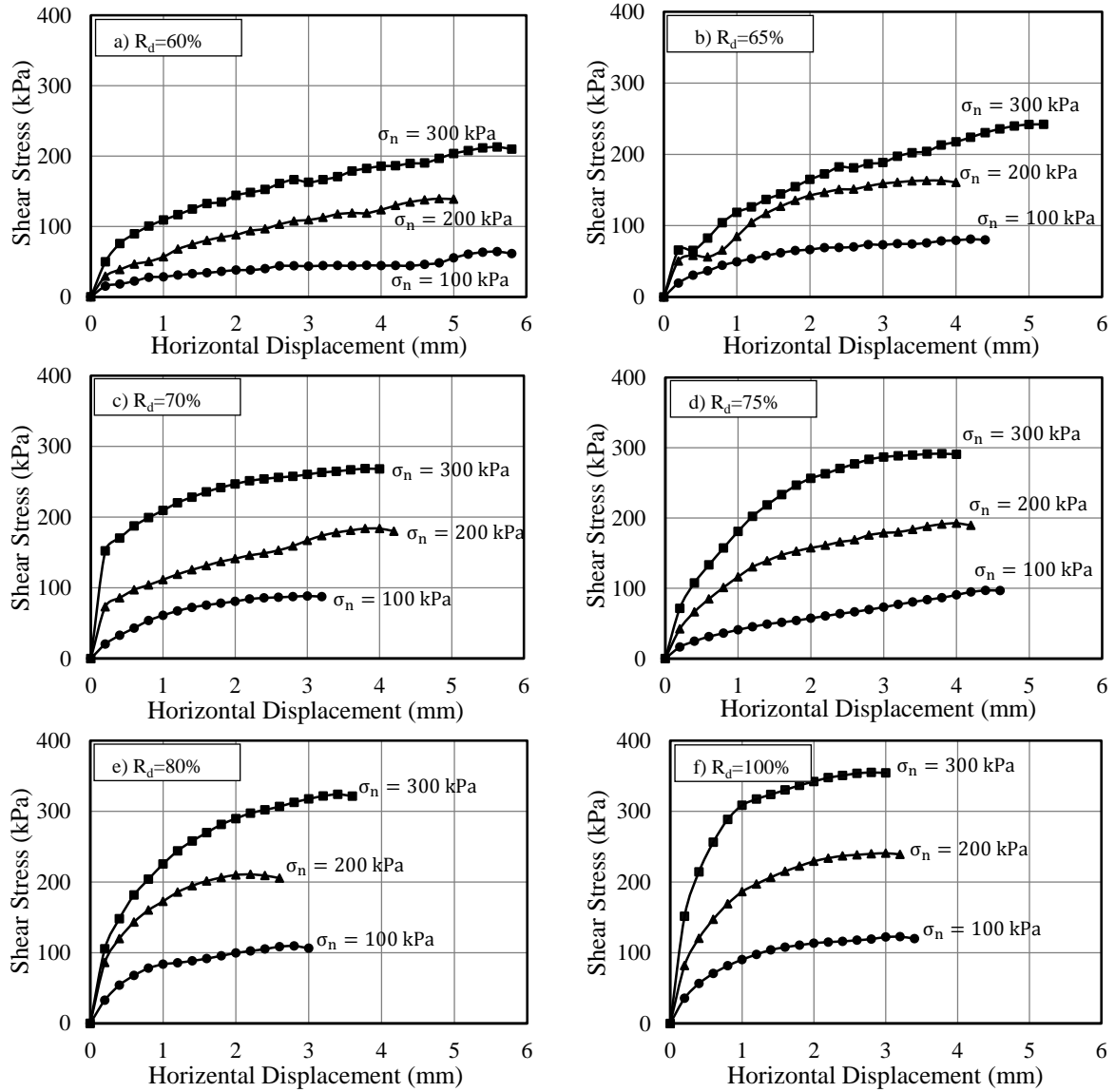
602  
603  
604  
605  
606

**Figure 5.** Shear stress-horizontal displacement of EPS block.



607  
608  
609  
610  
611  
612

**Figure 6.** Failure envelopes for EPS blocks.



613 **Figure 7.** Shear stress-horizontal displacement of sand at: a) 60%, b) 65%, c) 70%, d) 75%, e) 80% and f) 100%  
 614 relative densities.  
 615

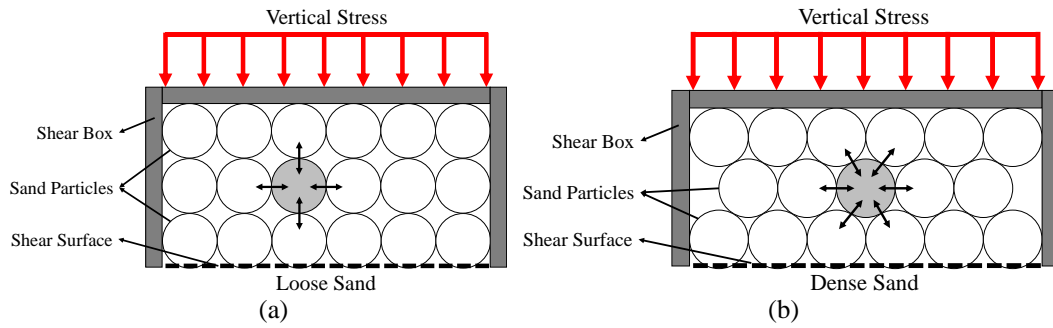
616

617

618

619

620



621 **Figure 8.** Comparison of intergranular points and confinements in direct shear test: a) idealized loose and b) dense  
 622 sand.  
 623

624

625

626

627

628

629

630

631

632

633

634

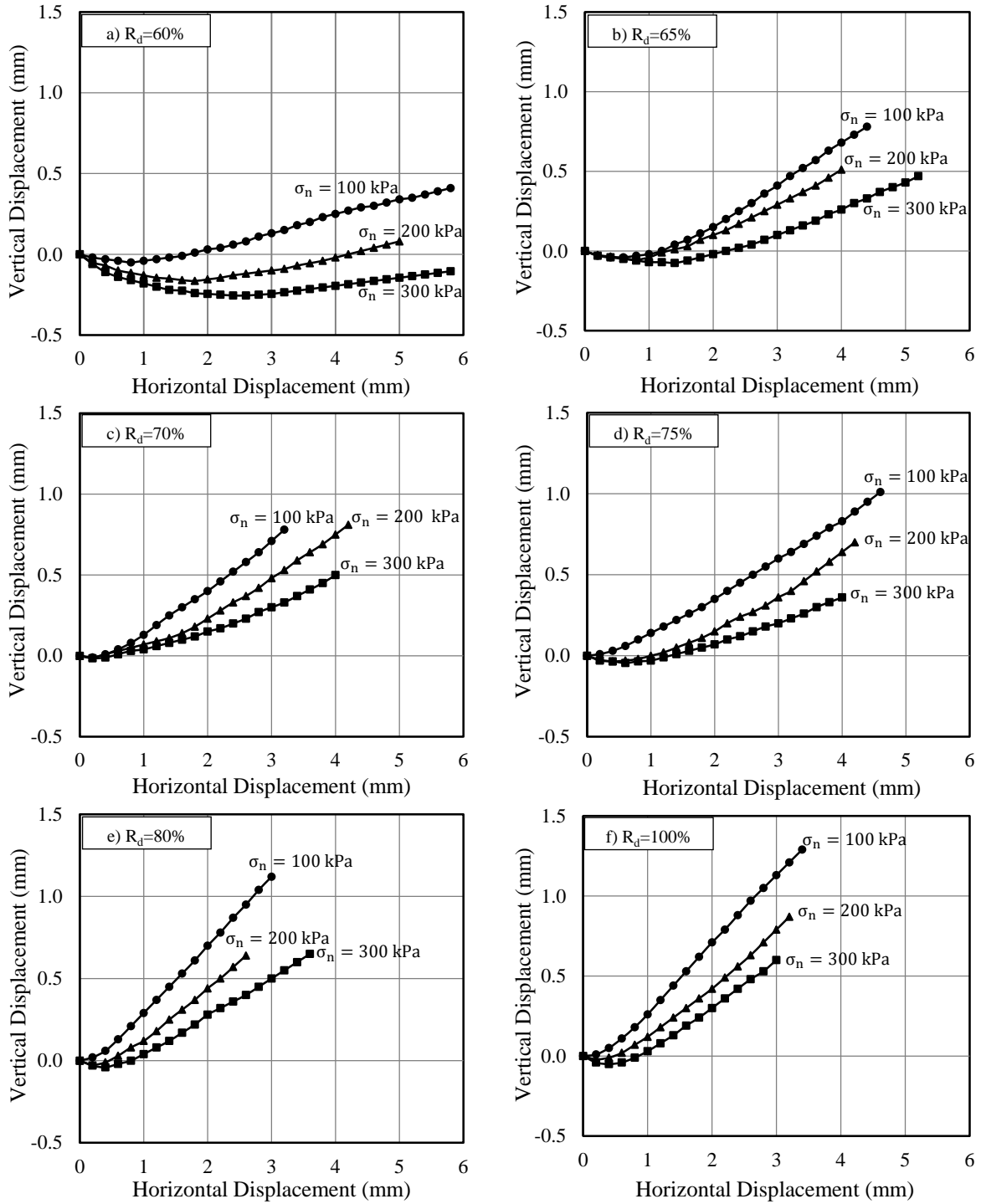
635

636

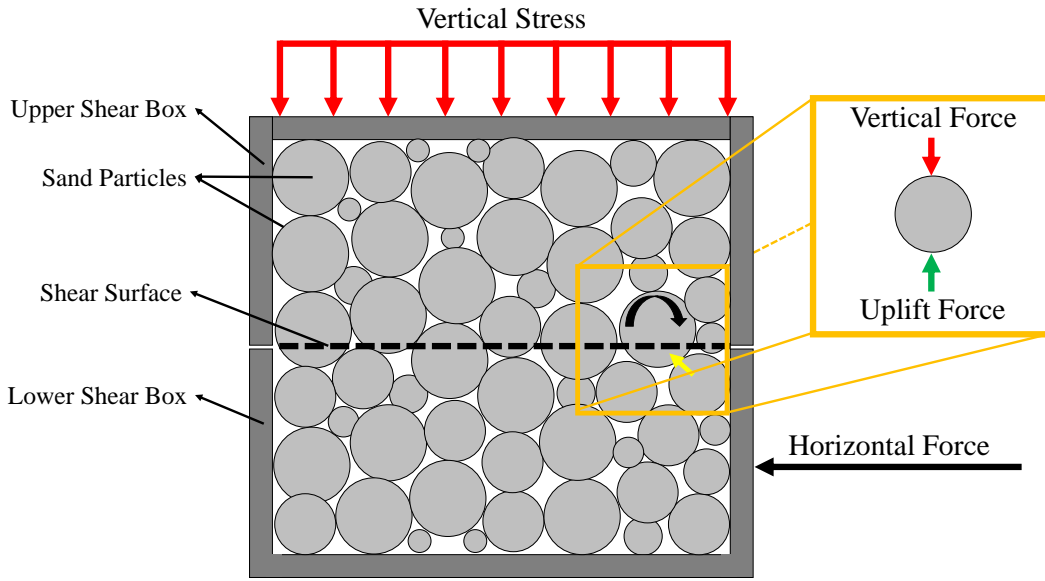
637

638

639

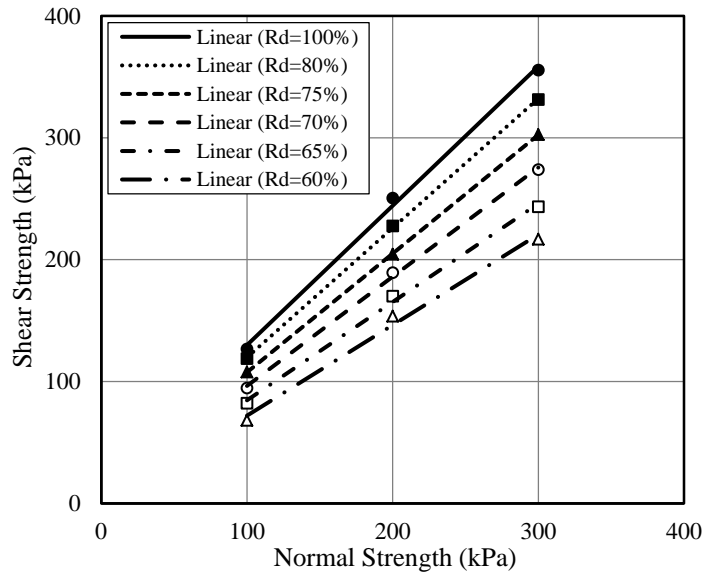


640 **Figure 9.** Vertical versus horizontal displacements of sands at: a) 60%, b) 65%, c) 70%, d) 75%, e) 80% and f)  
 641 100% relative densities.  
 642



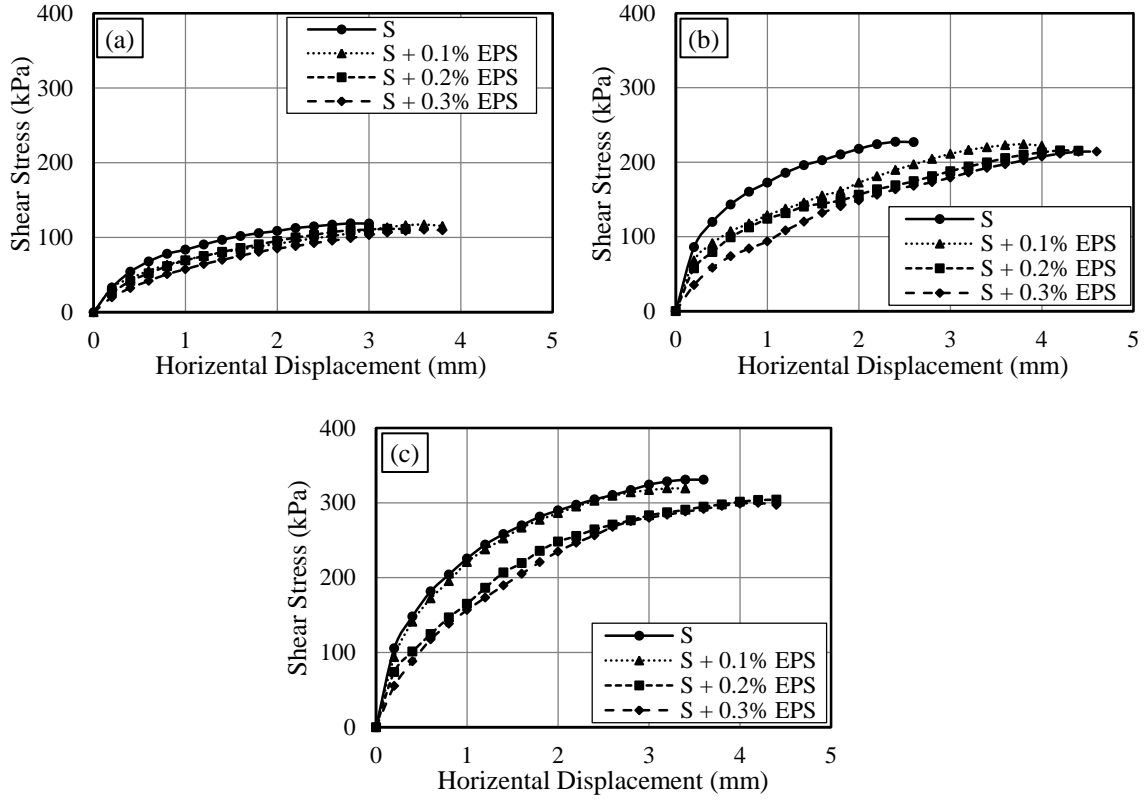
643  
644 **Figure 10.** Interaction of normal pressure and uplift forces on sand grains during shearing.  
645

646  
647



648  
649 **Figure 11.** Failure envelopes for sands with different relative densities.  
650





651 **Figure 12.** Shear stress-horizontal displacement of sand-eps particulate mixtures with  $R_d=80\%$ ; a)  $\sigma_n=100$  kPa, b)  
 652  $\sigma_n=200$  kPa, c)  $\sigma_n=300$  kPa.

653

654

655

656

657

658

659

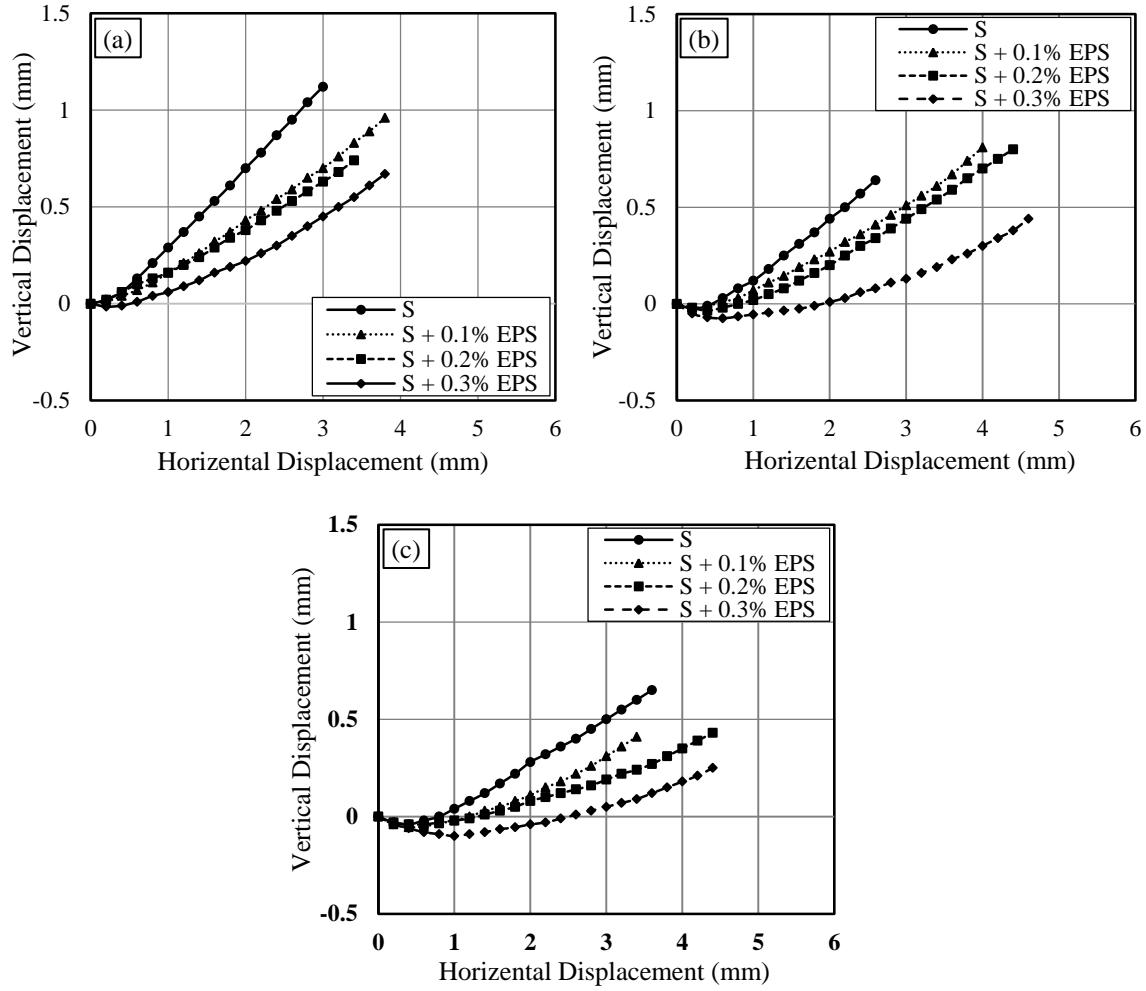
660

661

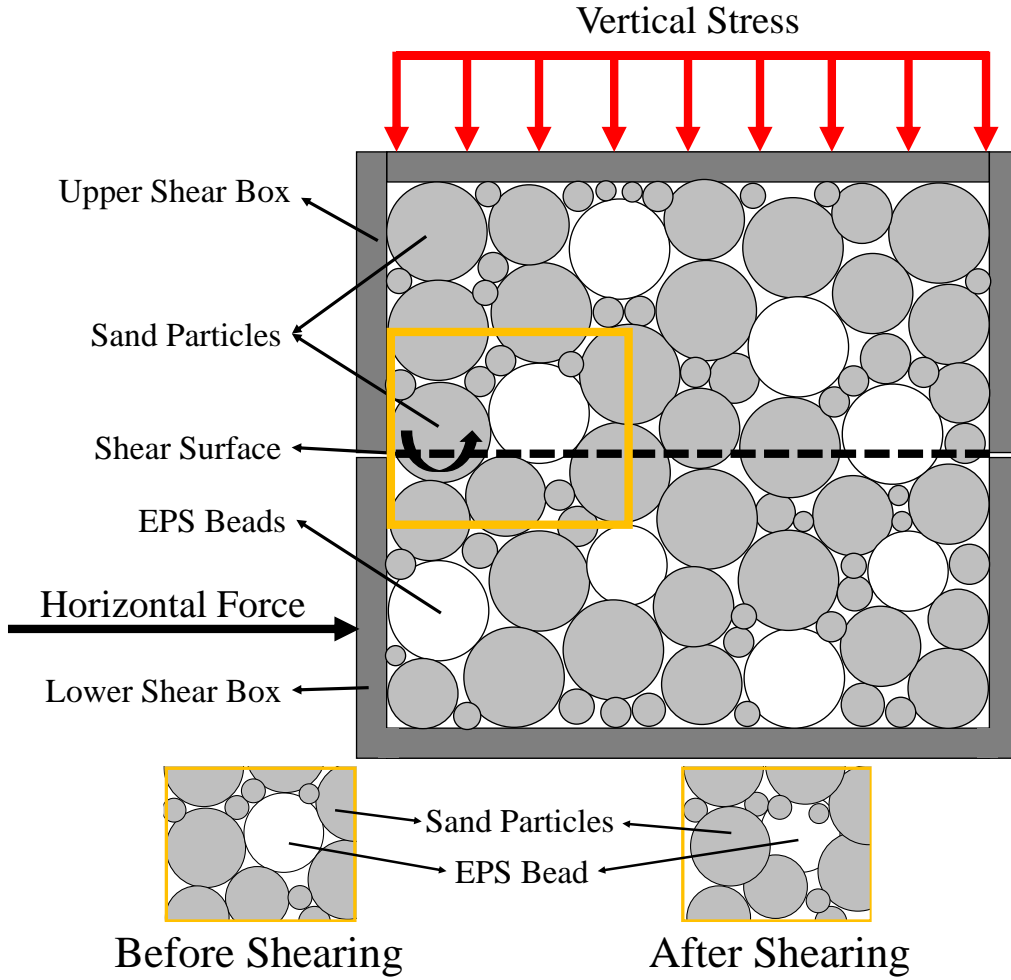
662

663

664



665 **Figure 13.** Vertical-Horizontal Displacement of sand-EPS mixtures with  $R_d=80\%$ ; a)  $\sigma_n=100$  kPa, b)  $\sigma_n=200$  kPa,  
 666 c)  $\sigma_n=300$  kPa.  
 667



668

669

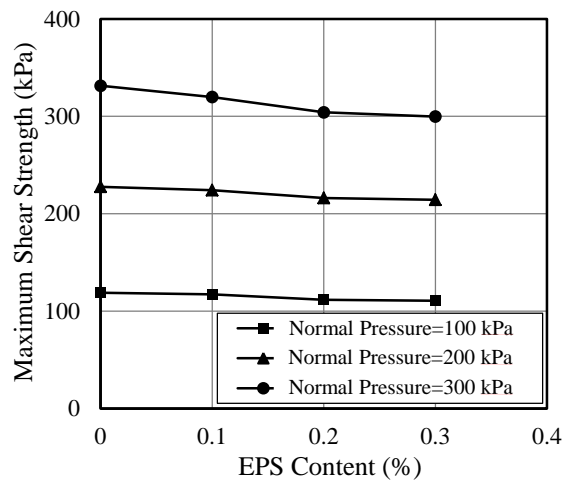
670

671

672

673

**Figure 14.** Position of sand and EPS particles before and after shearing.

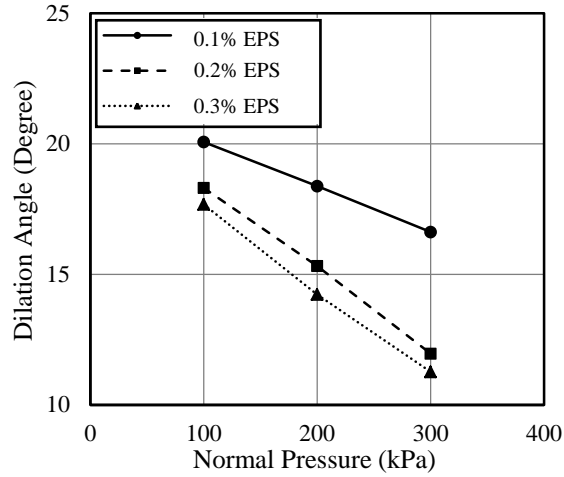


674

675

676

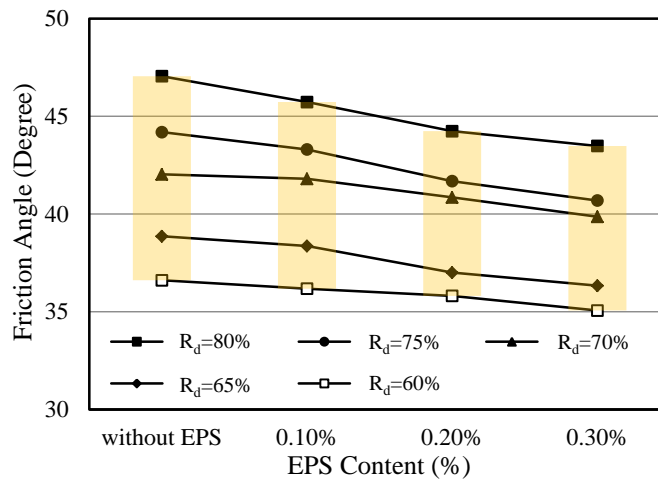
**Figure 15.** Variations of maximum shear strength-EPS content in mixtures with  $R_d=80\%$ .



677  
678 **Figure 16.** Dilation angle-normal pressure for sand-EPS mixtures with  $R_d=80\%$ .  
679

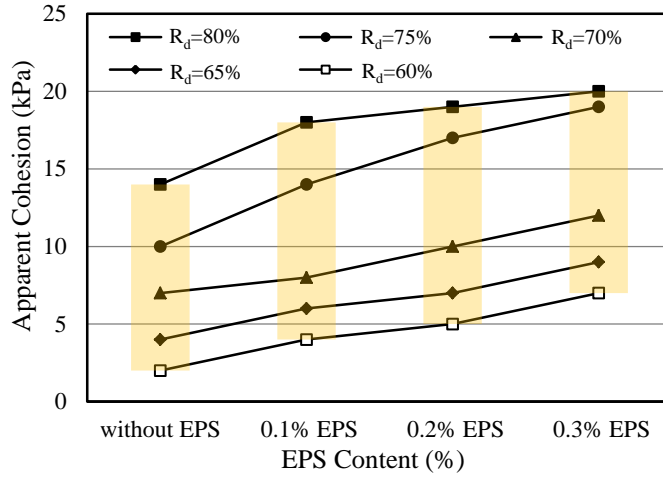
680

681



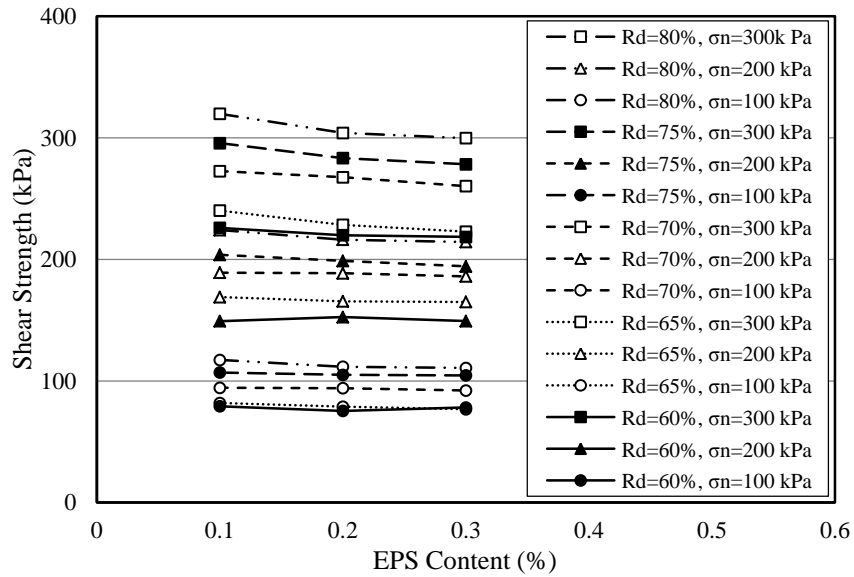
682  
683 **Figure 17.** Friction angle-EPS content in mixtures with different relative densities.  
684

684

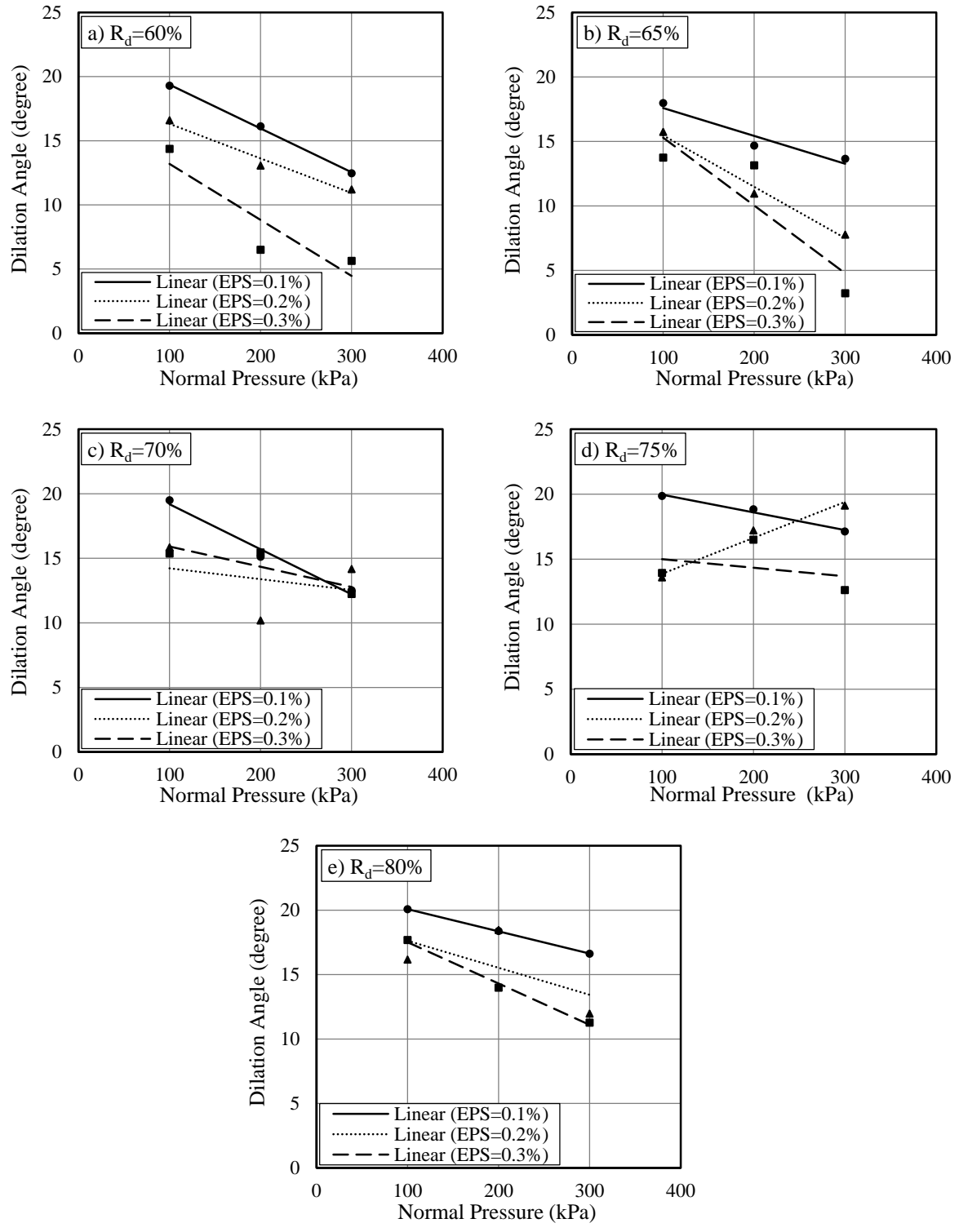


685  
686 **Figure 18.** Apparent cohesion-EPS content in mixtures with different relative densities.  
687

688  
689  
690



691  
692 **Figure 19.** Shear Strength-EPS content of all mixtures.  
693



694 **Figure 20.** Variations of dilation angles for sand-EPS mixtures of different densities subjected to  $\sigma_n=100, 200$  and  
 695 300 kPa.  
 696

697

698 **Tables:**

699 **Table 1.** Sand characteristics

700

Characteristics	Standard	Value
Max. dry unit weight, $\gamma_{max}$ (kN/m <sup>3</sup> )	ASTM D4253-16 [62]	15.43
Min. dry unit weight, $\gamma_{min}$ (kN/m <sup>3</sup> )	ASTM D4254-16 [63]	13.04
D <sub>10</sub> (mm)		0.36
D <sub>30</sub> (mm)		0.96
D <sub>60</sub> (mm)	ASTM D422-63 [65]	2.10
Coefficient of uniformity, $C_u$		5.83
Coefficient of curvature, $C_c$		1.22
USCS		SP

701

702

703

704

705

706

707

708

709 **Table 2.** Physical and mechanical properties of EPS particulates

710

Characteristics	Value
Density (kg/m <sup>3</sup> )	12.0
Compressive strength at 1% strain (kPa)	15
Compressive strength at 5% strain (kPa)	35
Compressive strength at 10% strain (kPa)	40
Flexural strength (kPa)	69
EPS particulate size (mm)	2-5

711

712

713

714

715

716

717

718 **Table 3.** Sand-EPS particulate mixtures investigated

R <sub>D</sub> (%)	EPS (%)	Total mass (g)	Mass of soil (g)	Mass of EPS (g)
100	0.0	147.23	-	-
	0.1		117.67	0.11
80	0.2	117.78	117.55	0.23
	0.3		117.43	0.35
	0.1		110.29	0.13
75	0.2	110.42	110.20	0.22
	0.3		110.09	0.33
	0.1		102.96	0.10
70	0.2	103.06	102.85	0.21
	0.3		102.75	0.31
	0.1		95.61	0.09
65	0.2	95.7	95.51	0.19
	0.3		95.42	0.28
	0.1		88.15	0.08
60	0.2	88.23	88.06	0.17
	0.3		87.97	0.26

719

720 **Table 4.** Shear strength parameter for EPS blocks

Test No.	$\Phi$ (degree)	C (kPa)
Test 1	2.8	18.6
Test 2	2.9	17.7
Test 3	2.9	17.7

721

722

723 **Table 5.** Summary of direct shear test conducted on EPS blocks

Reference	Sample size (mm×mm× mm)	Density (kg/m <sup>3</sup> )	Normal stress (kPa)	Shear strength parameters	
				$\Phi$ (degree)	C (kPa)
Padade and Mandal (2012) [69]	100×100×50	15 to 3	15 to 60	3 to 6	30.75 to 59.75
Özer and Akay (2016) [35]	Upper box: 100×100×25	18.4 and 28.8	10 to 40	8.9 to 10	26.2 to 49.8
	Lower box: 150×100×25				
AbdelSalam and Azzam (2016) [36]	100×100×50	20	10 to 40	Dry: 19 Wet: 33	Dry: 16 Wet: 12
Khan and Meguid (2018) [37]	100×100×40	15 to 35	18 to 54	9 to 10.5	28 to 55

724

725

726

727 **Table 6.** Summary of sand shear strength parameters at different relative densities

$R_d$ (%)	$\Phi$ (degree)	C (kPa)
100	49	16
80	47	14
75	44	10
70	42	7
65	39	4
60	37	2

728

729

730

731

732

733

734

735

736

737

738

739



740 **Biographies**

741 • **Mahmood Reza Abdi** obtained his MSc and PhD degrees from Bradford University and the University of  
742 South Glamorgan, UK, respectively. He is currently an Associate Professor and the Head of the Soil  
743 Mechanics Laboratory at Faculty of Civil Engineering, K.N. Toosi University of Technology, Tehran, Iran.  
744 He has published many research articles on soil improvement in national and international journals and  
745 supervised many students of MSc and PhD during his career.

746  
747 • **Ali Khakbazan** is working as an Assistant Professor at Department of Water-Soil Engineering, Imam  
748 Khomeini Higher Education Center, Karaj, Iran. He obtained his MSc and PhD degrees from Loughbrough  
749 and South Glamorgan Universities, UK, respectively. His main field of expertise is soil improvement and  
750 has taken part and supervised many geotechnical projects.

751  
752 • **Maryam Kazemi Abyaneh** obtained her BSc and MSc degrees in Civil Engineering and Geotechnical  
753 Engineering from K.N. Toosi University of Technology in 2017 and 2019, respectively. Her research  
754 interest is soil-geosynthetics interaction under pullout and direct shear modes. She is currently working in a  
755 geotechnical engineering company supervising various geotechnical projects.

756  
757 • **Mahdi Safdari Seh Gonad** obtained his Bachelor of Science in Civil Engineering from Ferdowsi  
758 University of Mashhad in 2015 and subsequently achieved his Master of Science in Geotechnical  
759 Engineering from K.N. Toosi University of Technology in 2017. Following his academic achievements, he  
760 has been engaged in research and has served as a research assistant in the Soil Mechanics Laboratory at  
761 K.N. Toosi University of Technology in Tehran, Iran. He is particularly interested in geotechnical  
762 engineering specially soil improvement techniques such as soil-reinforcement and deep soil mixing.

763